WORLD CONFERENCE ON TIMBER ENGINEERING 2025
BRISBANE, AUSTRALIA
Advancing Timber for the Future Built Environment

EXPERIMENTAL INVESTIGATION OF SLOTTED-IN PLATE MOMENT CONNECTIONS IN TIMBER FRAME BUILDINGS

Elif Appavuravther[1], Jose Henriques [2], Bram Vandoren[3]

ABSTRACT: In the past decades, the number of research work explaining the load transfer mechanism of moment connections has increased due to their advantages of energy dissipation capacity and improved load distribution. The use of bolts in slotted-in plate moment connections is a common practice in timber construction. However, the design and application guidelines are still limited and leading to results which deviate from experimental observations. In this paper, bolted slotted-in plate moment connections with multiple configurations are experimentally investigated. The results are used to verify the FprEN 1995-1-1 equations and to investigate the service conditions. First, shear tests on a single bolt – inserted in a glulam member – are conducted followed by single moment connection and then by a double moment connection. The experimental observation showed that the connections are controlled by the fastener behaviour, therefore an accurate analytical prediction is necessary. The results are compared with the rigid model, which is an extension of the European Yield Model. The deviations has shown the need for an improved analytical model.

KEYWORDS: bolted connection, moment-resisting connections, timber frames

1 – INTRODUCTION

With the 2050 Paris agreement, the carbon emission must be dramatically reduced by 2050. The use of timber in construction sector is in demand due to its environmentally friendly nature. The wood obtained by its natural form contains defects such as knots and the grain directions which reduce the mechanical performance of the material. With fabricated engineered wood products such as glue laminated timber (glulam), a less variable product behaviour across lamelas can be obtained.

With an increase in the mass timber construction, it has become crucial to understand the behaviour of structural connections [1]. In order to accommodate free spans designs and to ensure a robust structural system, moment-resisting connections, which can partly replace wall diaphragms, can play a key role in such designs [2].

In multi-storey timber buildings, including large spans, the use of glulam with slotted-in steel plate are a common approach to realise the connection between structural members such as beams and column [3-5]. Multiple dowel-type connections are preferred for moment connections as they can contribute to the axial resistance, shear and moment resistance [6]. The strength and the stiffness capacity of moment-resisting connections depend on the mechanical and in particular the shear behaviour of a single dowel connection. In the current EN 1995-1-1, the performance of such a connection can be determined using the European Yield model (EYM) [7]. In moment connections, apart from the individual connection behaviour, brittle failure modes of the timber member should be considered too as this behaviour is commonly observed in the literature [3, 8, 9].

In this paper, a multiscale experimental approach is performed, in which, first the shear behaviour of a single bolt (embedded in a glulam member) was investigated, then upscaled towards an entire moment connection (with different configurations) and subsequently upscaled to a joint consisting of two such moment

[1] Elif Appavuravther, UHasselt, Faculty of Engineering Technology, Construction Engineering Research Group (CERG), Agoralaan, 3590 Diepenbeek, Belgium, eliftuba.appavuravther@uhasselt.be

[2] Jose Henriques, UHasselt, Faculty of Engineering Technology, Construction Engineering Research Group (CERG), Agoralaan, 3590 Diepenbeek, Belgium, jose.gouveiahenriques@uhasselt.be

[3] Bram Vandoren, UHasselt, Faculty of Engineering Technology, Construction Engineering Research Group (CERG), Agoralaan, 3590 Diepenbeek, Belgium, bram.vandoren@uhasselt.be

https://doi.org/10.52202/080513-0535

connections. The experimental observations are reported and comparison is made with the analytical calculations according to FprEN 1995-1-1 [10]. The rigid model approach is used to determine the strength and the stiffness of the moment-resisting connections [11]. The deviations at the single connection and multiple connection level are discussed. The conservative assumptions of the method are identified.

2 – ANALYTICAL APPROACH

In the Eurocode 5 design standard FprEN 1995-1-1 [10], the included EYM is based on the Johansen's yield theory [12]. The code identifies that four failure modes can occur for symmetric connections including a central steel plaat, with a fastener loaded in double shear. These failure modes are:

i. Crushing of the timber layer, mode a (F_a),
ii. Crushing of the steel layer, mode b (F_b),
iii. Single plastic hinge formation at the central element, mode d (F_d)
iv. Double plastic hinge formation at the central element and side elements, mode f (F_f).

These modes are referred to as the dowel effect contribution, $F_{D,k}$. The strength is governed by the minimum failure mode capacity:

$$F_{D,k} = \min\{F_a, F_b, F_d, F_f\} \quad (1)$$

In failure mode d and f, with yielding of the fasteners, the rope effect, $F_{rp,k}$, is activated which contributes to the strength of the connection. The rope effect is the minimum of design tensile resistance (which is the minimum of head pull-through resistance, withdrawal resistance and tensile resistance of the fastener), with a reduction factor of 25% and characteristic dowel effect contribution. Both the dowel effect and rope effect constribution is summed to determine the capacity of a connector referred to as lateral resistance per shear plane, $F_{v,k}$,:

$$F_{v,k} = F_{D,k} + F_{rp,k} \quad (2)$$

Due to symmetry and the steel-to-timber connection the lateral resistance must be doubled [10]. The stiffness, referred to as slip modulus, of a single bolt per shear plane, k_{ser}, is determined by (3):

$$k_{ser} = \rho_{mean}^{1.5} d/23 \quad (3)$$

With ρ_{mean} representing the mean density of wood and d is the nominal diameter of the fastener. Once again, due to symmetry and steel-to-timber connection, the stiffness must be doubled [10]. In FprEN 1995-1-1, a clause for fasteners loaded perpendicular to the grain is added, which suggests the slip modulus to be reduced by 50% [10].

In the design codes, an analytical model to predict moment-resisting connections is not covered. Porteous and Kermani [11] extended the EYM for multiple dowel connections and referred to it as the rigid model approach. In this model: i) the material between the fasteners is assumed to be rigid, ii) the center of rotation is at the centroid of the fasteners, iii) the center of rotation remains constant, iv) the load distribution is proportional to the center of rotation and v) the bending moment resistance is the result of the sum of the contribution of each indivual fastener/bolt. The largest strength of the connection, $F_{d,i}$, is determined from the vector sum of the forces:

$$F_{d,i} = \sqrt{\left(F_{v,d,i} + F_{m,d,i}\cos\beta\right)^2 + \left(F_{h,d,i} + F_{m,d,i}\sin\beta\right)^2} \quad (4)$$

With $F_{v,d,i}$, $F_{m,d,i}$, and $F_{h,d,i}$ being the shear force, moment force and axial force per bolt, respectively and β being the angle of the bolt from the centroid of the connection. Fom the horizontal axis, $F_{d,i}$ is determined with angle α:

$$\alpha = \arccos\left(\frac{F_{h,d,i} + F_{m,d,i}\sin\beta}{F_{d,i}}\right) \quad (5)$$

The joint stiffness, K_J, is:

$$K_J = k_{ser}\sum_{i=1}^{n} r_i^2 \quad (6)$$

which is a function of the bolt radius, r_i.

3 – MATERIALS AND METHODS

3.1 TEST SPECIMENS AND DESIGN

In this study, moment connections are experimentally investigated. Within the experimental campaign, the connection is tested at different scales to observe the impact from the connector level to a full-scale frame building, as given in Figure 1. At the connector level, a single threaded rod is tested under shear loading, both parallel, ST-0, and perpendicular, ST-90, to the grain configuration. The specimen dimensions are presented in Figure 2. At the joint level, a single moment-resisting connection, MR-1 and a double moment-resisting connection, representing column-beam joint, MR-2 are tested. The elements are designed for the threaded rods to yield, forming a double hinge, as idealised by failure mode f as described in the previous section. The moment-resisting connection is designed to resist service loads of a 6 m frame span, which resulted in 38 threaded rods,

https://doi.org/10.52202/080513-0535

with 22 on the outer circle and 16 in the inner circle. Details are given in Figure 3. The dimensions of MR-2, the column-beam joint, are presented in Figure 4. In the inner and outer circle, the threaded rods are distributed among a circle diameter of 300 mm and 420 mm, respectively.

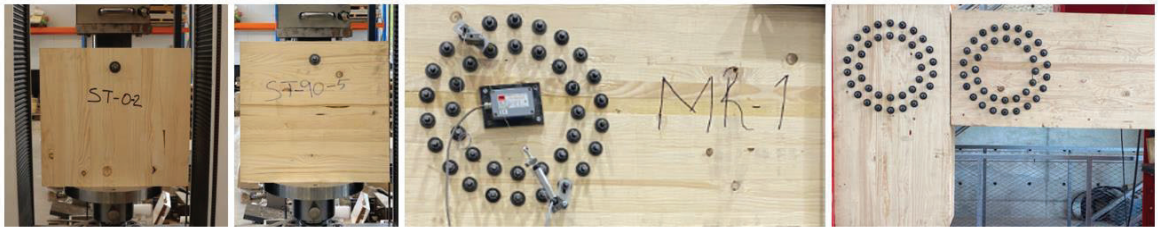

Figure 1: Test specimens, from left to right: (a) Shear test where the threaded rod is parallel to the grain, ST-0; (b) Shear test where the threaded rod is perpendicular to the grain, ST-90; (c) Single moment connection, MR-1; (d) Column-beam moment connection, MR-2.

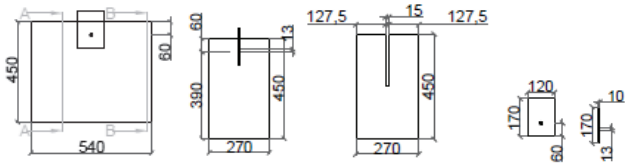

Figure 2: Specimen dimension of the shear tests (same for both ST-0 and ST90), from left to right: (a) Front viewy; (b) Cross-section A-A; (c) Cross-section B-B; (d) Front view of the steel plate; (e) Side view of the steel plate. All dimensions are in millimeters.

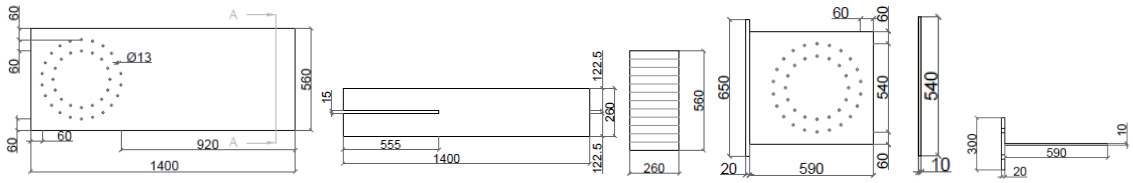

Figure 3: MR-1 specimen dimensions, from left to right: (a) Front view of the timber beam; (b) Top view of the timber beam; (c) Cross-section of the timber beam; (d) Front view of the steel plate; (e) Cross-section of the steel plate;(f) Top view of the steel plate. All dimensions are in millimeters.

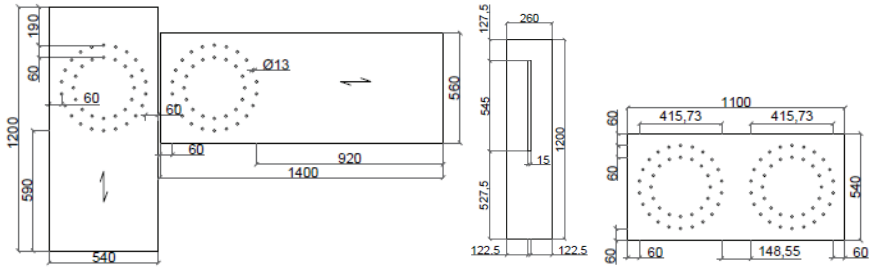

Figure 4: MR-2 specimen, from left to right: (a) Front view of column-beam joint; (b) Side view of the column; (c) Front view of the steel plate. All dimensions are in millimeters.

3.2 MATERIALS

The timber used in the experimental campaign has a strength class of GL 24h with an average humidity of 12.2% and density of 434 kg/m^3 (measured from 10 random specimens which were located in an uncontrolled indoor environment). The slotted-in steel is made of S235 steel. The fasteners consist of 12 mm diameter fully threaded rods with a strength class of 8.8 installed with washer and nut on both ends.

3.3 TEST SETUP, MONITORING AND TEST PROCEDURE

The shear tests are conducted using a Dartec tensile machine with capacity of 250 kN, given in Figure 5(a). The connector slip corresponds to the settlement between the cylinders.

The experimental setup for the bending tests contains a frame, a hydraulic jack, a load cell and LVDTs (Linear Variable Differential Transformers). In Figure 5(b), the test instrumentation for MR-2 is presented. The same instrumentation scheme is used for MR-1 with measurement devices limited to X1-X10. In MR-1 six LVDTs measured the vertical displacement along the length of the beam (X1 – X5 and X10), one out of plane (X6), one measured the sway of the experimental frame (X8) and a wire was placed between two extreme threaded rods to measure the distance changes of the threaded rods (X9). Lastly, an inclinometer was placed at the center of the threaded rods to measure the rotation of the element (X7). In MR-2, four more sensors are added to measure the column sway (X11), column rotation (X12), distance between the threaded rods (X13) and the vertical displacement on the column (X14). Additionally, the moment connections are monitored with a Digital Image Correlation (DIC) system to analyse the local and global deformations.

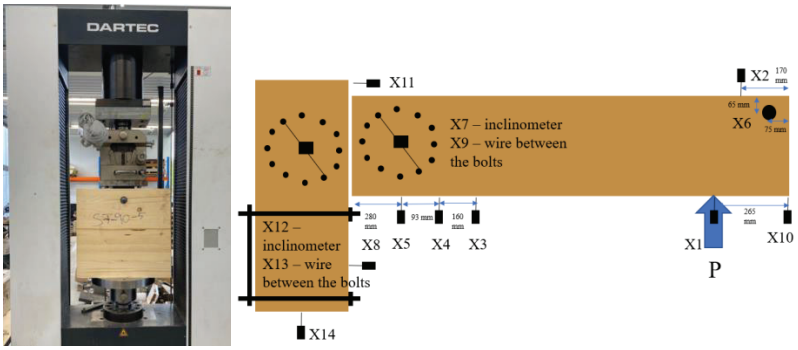

Figure 5: From left to right (a) Test setup of the shear tests; (b) Instrumentation of MR-2.

4 – RESULTS, DISCUSSIONS AND COMPARISON WITH ANALYTICAL MODELS

4.1 SHEAR CONNECTIONS

In Figure 6, force-slip curves of all five replicas are presented along with analytical predictions based on FprEN 1995-1-1 [10]. The load capacity is determined by the maximum load reached by a connection or by the load corresponding to 30 mm of slip (for the cases loaded perpendicular to the grain), depending on which is reached first. The yield load is determined using EN 12512 [13]. The stiffness of the connector is determined using EN 26891 [14] as the ratio of force to slip at 40% to 10% of load capacity in the initial loading phase.

In both series, the replicas followed a similar trend. In the linear range, a constant stiffness is recorded until the dowel effect is reached. After this load level, the rope effect is activated, caused by head pull through resistance of the washer.

In the series where load is applied parallel to the grain, ST-0, the ultimate load capacity is reached due to tension failure of the threaded rods, causing a drop in the load-capacity. The analytical prediction lead to a 137% overestimation of the stiffness, and 38% and 3% overestimation of the average load-carrying capacity for the dowel effect ($F_{D,k}$) and connector resistance ($F_{v,K}$), respectively.

In the series where load is applied perpendicular to the grain, ST-90, the ultimate load capacity is reached either due to tensile failure of the threaded rods or compression failure of the timber fibers under the threaded rods. The analytical prediction lead to an overestimation of 60% of the stiffness and to an underestimation of 69% of the dowel effect and 21% of the connector resistance.

https://doi.org/10.52202/080513-0535

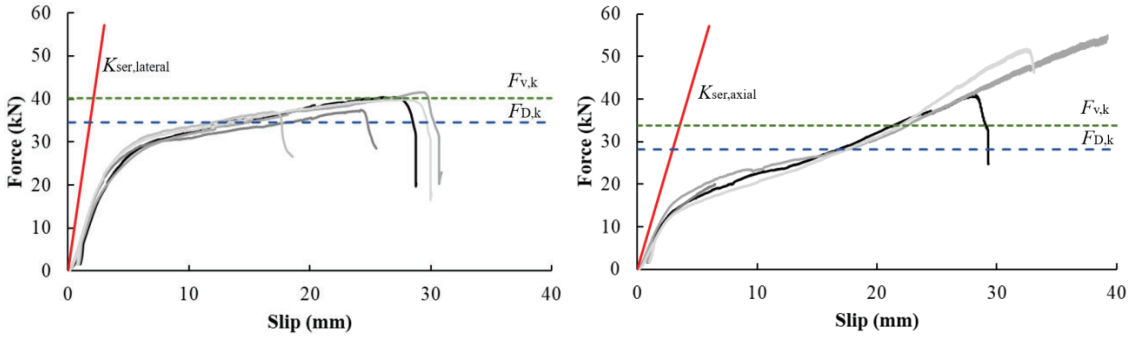

Figure 6: Shear test results with analytical predictions from FprEN 1995-1-1, from left to right: (a) Loading parallel to the grain; (b) Loading perpendicular to the grain.

4.2 MOMENT CONNECTIONS

In Figure 7, the moment-rotation curve of the joints MR-1 and MR-2 are presented, respectively. The figures also includes the joint rotational stiffness, K_J, and load corresponding to the first and all threaded rod failures as $F_{d,1}$ and $F_{d,all}$, respectively. In both test results, the initial slip caused due to loading against the gravity has been removed. The initial rotation is 0.273° which is the angle corresponding to 1 mm of slip at a radius of 210 mm (corresponding to the outer circular configuration). In MR-2, the initial rotation is assumed to be doubled and therefore, 0.546° is removed. The moment lever arm of MR-1 from load application point to the center of threaded rods was 1 m. The moment arm in MR-2 from loading point to the gap of column-beam joint was 1.225 m.

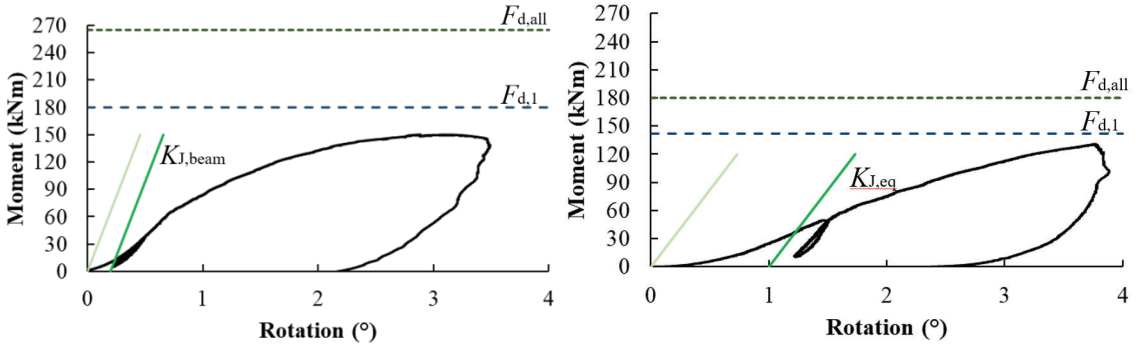

Figure 7: Bending test results with analytical predictions from FprEN 1995-1-1 (the stiffness line is shifted for easier recognition), from left to right: (a) MR-1 – single joint; (b) MR-2 – column-beam joint.

In MR-1, a linear stiffness is recorded until a load level of 65 kN, where yielding of the first set of threaded rods is expected. From 65 kN to 153 kN, a smooth plastic curve developed as threaded rods started yielding consecutively. At 153 kN the maximum load capacity is reached, F_{max}, due to tensile failure in the timber perpendicular to the grain. A picture of a failed specimen is presented in Figure 8, the crack is aligned with the last row of threaded rods.

The yielding of the first bolt in MR-1 is predicted as 180 kN by the rigid model approach, thus it overestimates by 177%. The failure of all threaded rods is predicted to occur at 265 kN. As the rigid model approach assumes an equal distribution of the loads among all threaded rods, if 177% is reduced from $F_{d,all}$, all threaded rods would yield at 95.67 kN. As the maximum load capacity is reached at 153 kN, it is likely that all threaded rods have rope effect activation. The analytical joint stiffness, K_J, is determined using Eq. (6). The new draft of FprEN 1995-1-1 [10] suggests that the stiffness can be reduced by 50% for bolts loaded perpendicular to the grain. For the intermediate angles, a linear interpolation may be applied [10]. The results showed that the analytical approach overestimated the stiffness by 195% (between the 10% to 40% of the maximum load capacity). This overestimation

https://doi.org/10.52202/080513-0535

is expected as at ST-90 shear tests (where the load was applied to perpendicular to the grain, see the previous section), a 60% overestimation was recorded. In the shear tests, five replicas were tested, and consistency among the replicas was observed. However, for the joint test, only one test was conducted which may not give an as accurate estimation.

Figure 8: Final failure of the MR-1 specimen due to a tensile crack perpendicular to the grain of the timber.

For MR-2, a linear behaviour is obtained until a load level of 55 kN (67 kNm). At this load level, the slope of the curve changed as it is expected that the bolts of the beam, that are aligned closest to the loading, have reached their elastic limit. The stiffness remained the same until 103 kN (126 kNm of moment). At this load level, the experiment had to be stopped as the stroke of the load cilinder was reached. No visual brittle fracture was observed.

In MR-2, the connections at the column and beam behave in serial rotational spring configuration, which results in equal force transfer between the column and the beam and the combined connection stiffness, $k_{J,eq}$, is determined as:

$$\frac{1}{k_{J,eq}} = \frac{1}{k_{J,beam}} + \frac{1}{k_{J,column}} \qquad (7)$$

Where the beam connection stiffness, $k_{J,beam}$, and the column connection stiffness, $k_{J,column}$, are both contributing to the column-beam joint. The beam connection stiffness is same as the one from the MR-1 joint. As each bolt is loaded in a different angle, a reduction factor with a maximum of 50% (for bolts loaded perpendicular to the grain), the column connection stiffness is almost equal to the beam connection stiffness.

According to the rigid model approach, the first set of threaded rods to fail are located at the outer circle of the column. At the column, the moment force is higher due to the longer lever arm. The predictions shows that the first yielding of a bolt will occur at 142 kN, in experiments, the change in the moment-rotation curve stiffness occurred at 55 kN, leading to a 158% overestimation of the analytical approach. It is predicted that all threaded rods will yield at 180 kN, and if a 158% reduction is applied, this brings the load level to 71 kN. At that load level, no change in the experimental graphs is observed. The column-beam stiffness is overestimating the experimental observation by 227%. Once again, the overestimation is in line with the shear tests, as the rigid model approach is based on the calculation of the stiffness of a single bolt.

The comparison with the rigid model approach has shown significant variations with the experimental results. The assumptions given in Section 2 expects higher values than in reality, therefore, it is not safe. To assess these assumptions, measurements were taken during the experiments (for the first three). To assess the rigidity of the material between fasteners (assumption i. in Section 2), a wire transducer was placed between two extreme threaded rods (X9 in Figure 5). The force-deformation distribution for this quantity is presented in Figure 9 for specimen MR-1. The joint remained in the elastic range until 65 kN, however, the deformation between the threaded rods is almost 1 mm at this load level.

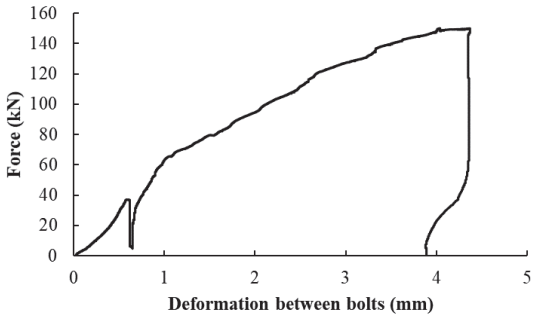

Figure 9: Distance evolution between extreme threaded rods for the MR-1 specimen.

The second assumption (the center of rotation is at the centroid of the fasteners) and the third assumptions (the center of rotation remains constant) are monitored using a DIC. In Figure 10, the overall displacement of MR-1 beam joint is presented for load levels of 5 kN and 20 kN. At 5 kN, which is during the early stage of the loading, the center of rotation of the joint was not at the center of the threaded rods, it was located 86 mm off. This observation aligns with the literature [15]. With the increase in force, the center of rotation changed even though the joint was exposed to the linear behaviour.

https://doi.org/10.52202/080513-0535

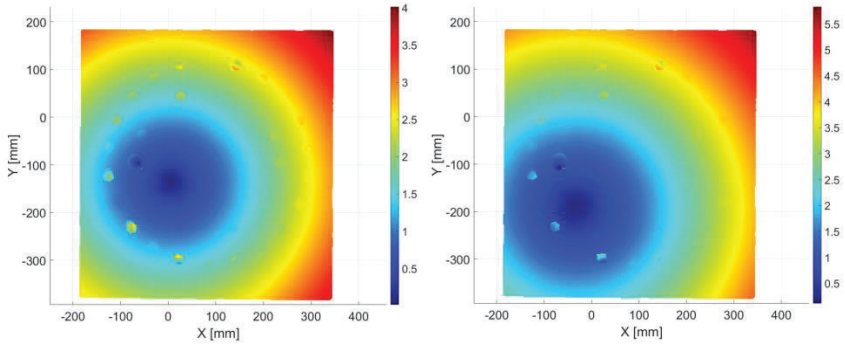

Figure 10: MR-1 DIC measurements (from left to right) at 5 kN and 20 kN.

5 – CONCLUSION

In this work, moment-resisting joints are experimentally analysed with slotted-in timber and fully threaded rods with washers and nuts. To characterise the joint accurately, shear tests were first conducted using a single threaded rod. Two different joint configurations are tested, a cantilever beam joint and column-beam joint. The test results are compared with the latest version of the Eurocode 5 design provisions, FprEN 1995-1-1. The deviations and assumptions are highlighted. The joints are analytically investigated by the rigid model approach which is an extension of the dowel connection in shear. This model is based on strict assumptions and the experimental investigation has shown that they are overconservative, which makes it unsafe to apply. As a result of this work, the need for an analytical model with a more realistic approach is crucial.

ACKNOWLEDGEMENTS

We would like to acknowledge the Flemish Agency for Innovation and Entrepreneurship (VLAIO) Technology Transfer Program (TETRA) for funding the HBC.2023.0066 HoP_HoVer project. The authors would like to thank Tine Engelen and Dan Dragan for their contributions to the experiments.

6 – REFERENCES

[1] COST, Design of connections in timber structures: A state-of-the-art report by COST Action FP 1402/WG3. 2018.

[2] A. Rebouças, Z. Mehdipour, J. Branco, and P. Lourenço, "Ductile Moment-Resisting Timber Connections: A Review," Buildings, 2022, doi: https://doi.org/10.3390/buildings12020240.

[3] M. Wang, X. Song, X. Gu, and J. Tang, "Bolted glulam beam-column connections under different combinations of shear and bending," Engineering Structures, 2019.

[4] A. Bouchaïr, P. Racher, and J. Bocquet, "Analysis of dowelled timber to timber moment-resisting joints," Materials and Structures, vol. 40, 2007, doi: DOI 10.1617/s11527-006-9210-0.

[5] R. Abrahamsen, "Construction of an 81 m tall timber building," 23. Internationales Holzbau-Forum IHF 2017, 2017.

[6] Z. Shu, Z. Li, Y. Xiangsheng, J. Zhang, and M. He, "Rotational performance of glulam bolted joints: Experimental investigation and analytical approach," Construction and Building Materials, vol. 213, 2019.

[7] EN 1995-1-1 - Design of timber structures - Part 1-1: General rules and rules for buildings, European Committee for Standardization, 2004.

[8] M. He, J. Zhang, and Z. Li, "Influence of cracks on the mechanical performance of dowel type glulam bolted joints," Construction and Building Materials, vol. 153, 2017.

[9] M. Schweigler, "Nonlinear modeling of reinforced dowel joints in timber structures - a combined experimental-numerical study," Doctor of Science, Civil Engineering, Vienna University of Technology, Vienna, 2018.

[10] FprEN 1995-1-1:2025 - Eurocode 5: Design of timber structures - Part 1-1: General rules and rules for buildings, 2025.

[11] J. Porteous and A. Kermani, Structural timber design to Eurocode 5. Oxford ; Malden, MA: Blackwell Pub., 2007, pp. xii, 542 p.

[12] K. Johansen, "Theory of timber connections," International association of bridge and structural engineering, vol. 9, pp. 249-262, 1949.

[13] EN 12512 - Timber structures - Test methods - Cyclic testing of joints made with mechanical fasteners, 2002.

[14] EN 26891 - Timber Structures - Joints Made with Mechanical Fasteners - General Principles for the Determination of Strength and Deformation Characteristics, 1991.

[15] V. Karagiannis, C. Malaga-Chuquitaype, and A. Y. Elghazouli, "Behaviour of hybrid timber beam-to-tubular steel column moment connections," Engineering Structures, vol. 131, 2017.

https://doi.org/10.52202/080513-0535